Imaging "Mini-Atlas" of Vascular Liver Diseases

"Mini-atlas" de Imagens em Doenças Vasculares do Fígado

Rita Trovisco[1], Manuela França[1,2]

Keywords: Hepatic Artery/diagnostic imaging; Liver Diseases/diagnostic imaging; Portal Vein/diagnostic imaging; Vascular Diseases/diagnostic imaging.

Palavras-chave: Artéria Hepática/diagnóstico por imagem; Doenças do Fígado/diagnóstico por imagem; Doenças Vasculares/diagnóstico por imagem; Veia Porta/diagnóstico por imagem.

Vascular liver diseases are a rare yet significant non-cirrhotic cause of portal hypertension. These conditions encompass a diverse group of conditions attributable to abnormalities in hepatic vascular inflow, sinusoidal circulation, or venous outflow. The liver's distinctive dual blood supply, primarily from the portal vein with a lesser contribution from the hepatic artery, is crucial in influencing the imaging characteristics of vascular liver diseases. A decrease in portal venous flow induces compensatory hyperperfusion of the hepatic artery, leading to characteristic perfusion patterns, vascular remodelling, and secondary morphological alterations.[1-3]

Imaging plays a crucial role in the assessment of vascular liver diseases. Ultrasound, particularly with Doppler evaluation, enables real-time assessment of vascular patency, flow direction, and haemodynamic changes. Contrast-enhanced computed tomography (CT) provides a comprehensive overview of vascular anatomy, liver morphology, parenchymal perfusion, collateral pathways, and related complications. Magnetic resonance imaging (MRI) offers vascular and perfusion assessment as well, with superior tissue characterisation, which might be advantageous in differentiating vascular disorders from other diffuse liver diseases. Furthermore, the use of hepatobiliary contrast agents is particularly advantageous for identifying and characterising associated benign hypervascular nodules and for distinguishing these hyperplasia-like nodules from malignant lesions.[3,4]

Unlike primary parenchymal liver diseases, vascular liver diseases are predominantly caused by hemodynamic disturbances rather than hepatocellular injury or fibrosis, particularly in the early stages. However, they frequently present with portal hypertension and morphological changes that can mimic liver cirrhosis in both clinical and radiological assessments. Accurate diagnosis is crucial, as management strategies, prognosis, and follow-up differ markedly from those of cirrhosis and other diffuse parenchymal liver diseases. Therefore, appropriate interpretation of imaging findings is essential to prevent misdiagnosis and to facilitate optimal patient management. ■

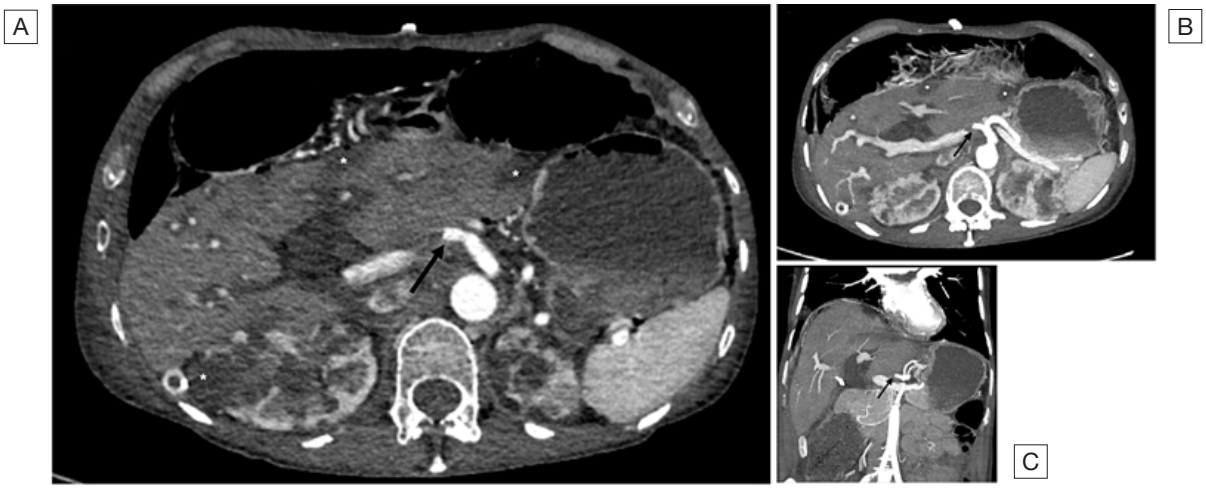

Figure 1: **Hepatic artery obstruction** following liver transplantation. Axial contrast-enhanced CT images during the arterial phase [**A**], along with axial [**B**] and coronal [**C**] maximum intensity projection (MIP) images, reveal occlusion (arrow) of the common hepatic artery, attributable to hepatic artery thrombosis. The enhancement of the hepatic parenchyma is heterogeneous, with peripheral wedge-shaped hypointensity areas in segments II and VII, extending to the capsular surface, due to hypoperfusion (*).

[1]Radiology Department, Hospital de Santo António, Centro Hospitalar Universitário de Santo António, ULS de Santo António (Santo António), Porto, Portugal
[2]Unit for Multidisciplinary Research in Biomedicine, School of Medicine and Biomedical Sciences, University of Porto, Porto, Portugal

https://doi.org/10.60591/crspmi.560

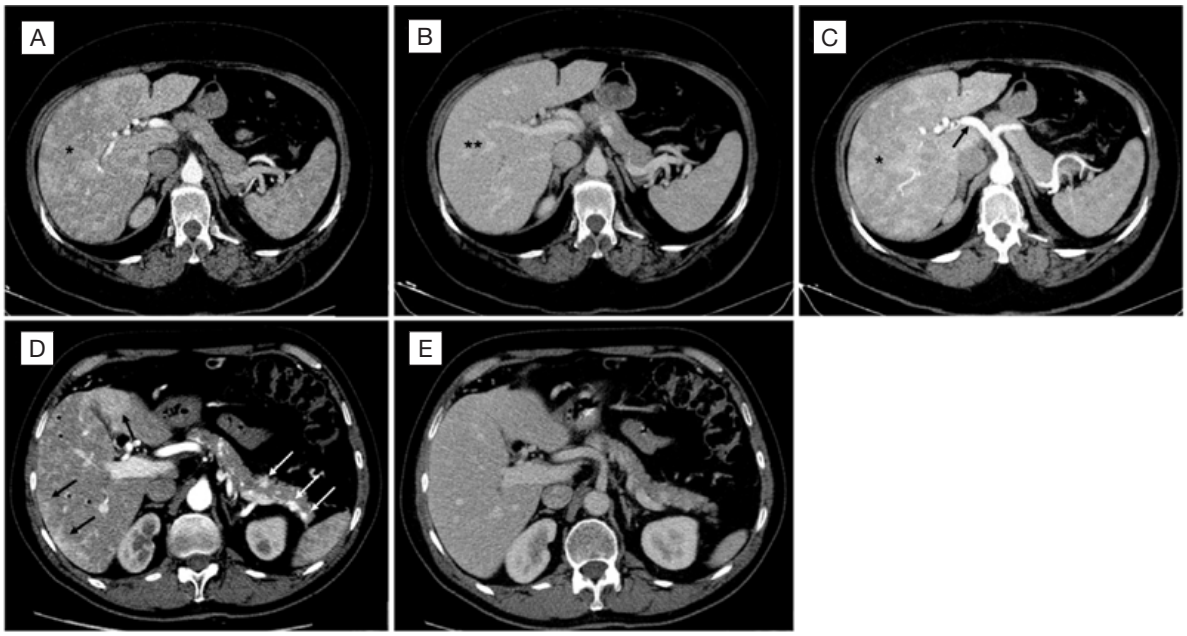

Figure 2: Liver involvement in hereditary hemorrhagic telangiectasia (HHT). Axial contrast-enhanced CT images in the arterial phase [**A**] demonstrate transient hepatic attenuation differences (THAD, *) likely related to telangiectasias and vascular shunts in the context of HHT. Axial contrast-enhanced CT images in the portal venous phase [**B**] show homogeneous hepatic parenchymal enhancement. Axial [**C**] arterial-phase maximum intensity projection (MIP) image depicts increased calibre of the hepatic artery (HA) due to liver hyperarterialization seen in HHT. [**D**] and [**E**], axial contrast-enhanced CT images of another patient with HHT. Hepatic arterial phase image [**D**] shows a prominent HA and wedge-shaped areas of hyperenhancement at the periphery of the liver (black arrows) related with THAD. Multiple telangiectasias are seen as small peripheral hypervascular areas (*). In addition, multiple vascular malformations are also depicted in the pancreas (white arrows). The portal venous phase image [**E**] shows homogenization of the liver parenchyma, with telangiectasias becoming isodense with the adjacent parenchyma.

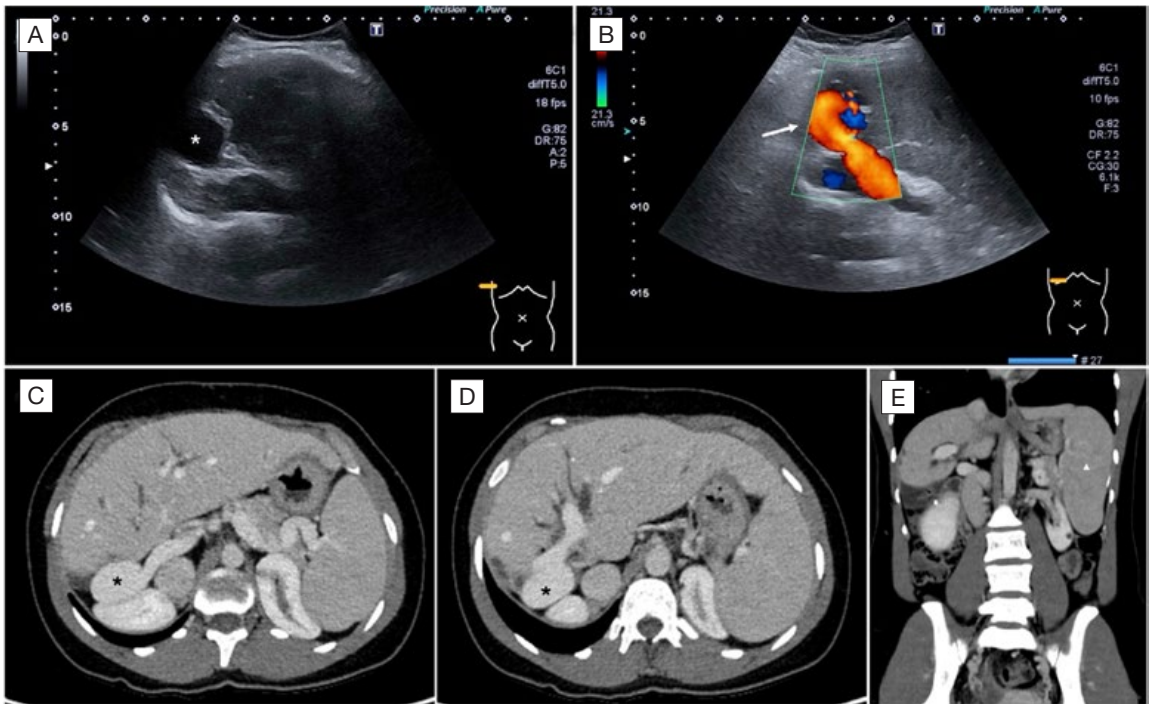

Figure 3: Portal vein aneurysm. B-mode ultrasound [**A***], and color Doppler ultrasound [**B**] arrow, demonstrate an aneurysm of the main portal vein in a post–liver transplant patient. Color Doppler shows multidirectional flow with the characteristic "yin-yang" sign [**B**]. Axial [**C** and **D**] and coronal [**E**] contrast-enhanced CT images in the portal venous phase confirm a saccular aneurysm of the main portal vein (*). The hepatic graft shows a globular morphology with left hepatic lobe hypertrophy, smooth but blunt contours, and homogeneous parenchymal enhancement. Splenomegaly (▲), related to portal hypertension, is also seen.

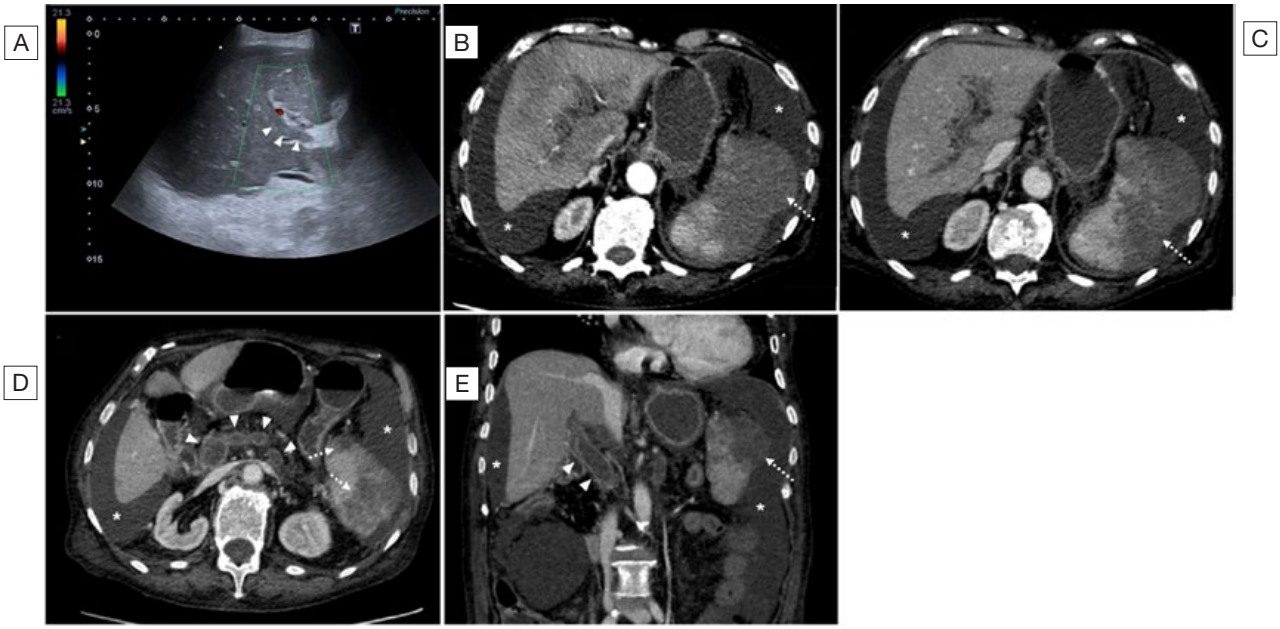

Figure 4: Acute portal and splenic vein thrombosis in a patient with primary myelofibrosis. Color Doppler ultrasound [**A**] shows no flow in the main portal vein, along with echogenic material inside the vessel, due to portal vein thrombosis (arrowheads). Axial [**B**] – hepatic arterial phase; [**C** and **D**] – portal venous phase and coronal [**E**] contrast-enhanced CT images reveal thrombosis of the splenoportal axis (arrowheads). On the hepatic arterial phase [**B**], the liver shows heterogeneous enhancement, becoming homogenous on the portal venous phase [**C**], indicating transient perfusion abnormalities related to portal vein thrombosis. Splenic infarcts are seen (dashed arrow). Ascites (*) is present, probably due to acute portal vein thrombosis.

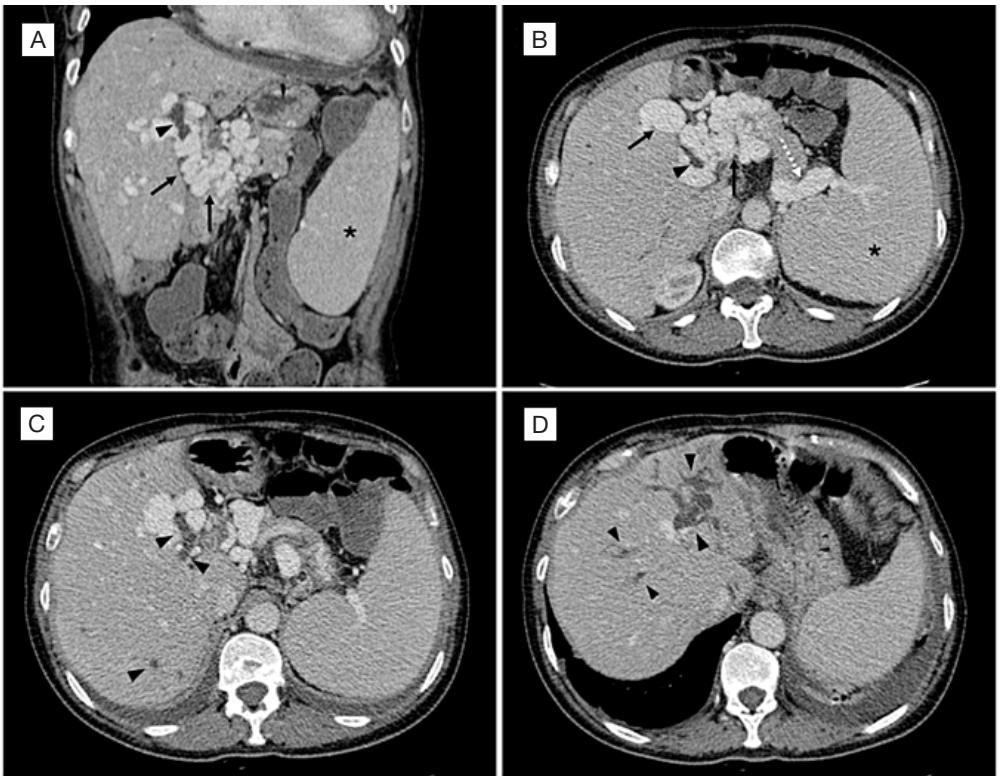

Figure 5: Portal cavernoma and biliary cholangiopathy in a woman with antiphospholipid syndrome and systemic lupus erythematosus, with a history of portal vein thrombosis 11 years earlier. Coronal [**A**] and axial [**B-D**] contrast-enhanced CT images in the portal venous phase demonstrate serpiginous porto-portal collateral vessels consistent with cavernous transformation of the portal vein (portal cavernoma) (arrows). The cavernoma causes extrinsic compression of the common bile duct (arrowhead in **B**), with upstream biliary dilatation (arrowheads in [**A**, **C**, and **D**], suggesting biliary cholangiopathy. Additional findings include splenic vein dilatation (dashed arrow in **B**) and splenomegaly [**A** and **B***], secondary to portal hypertension.

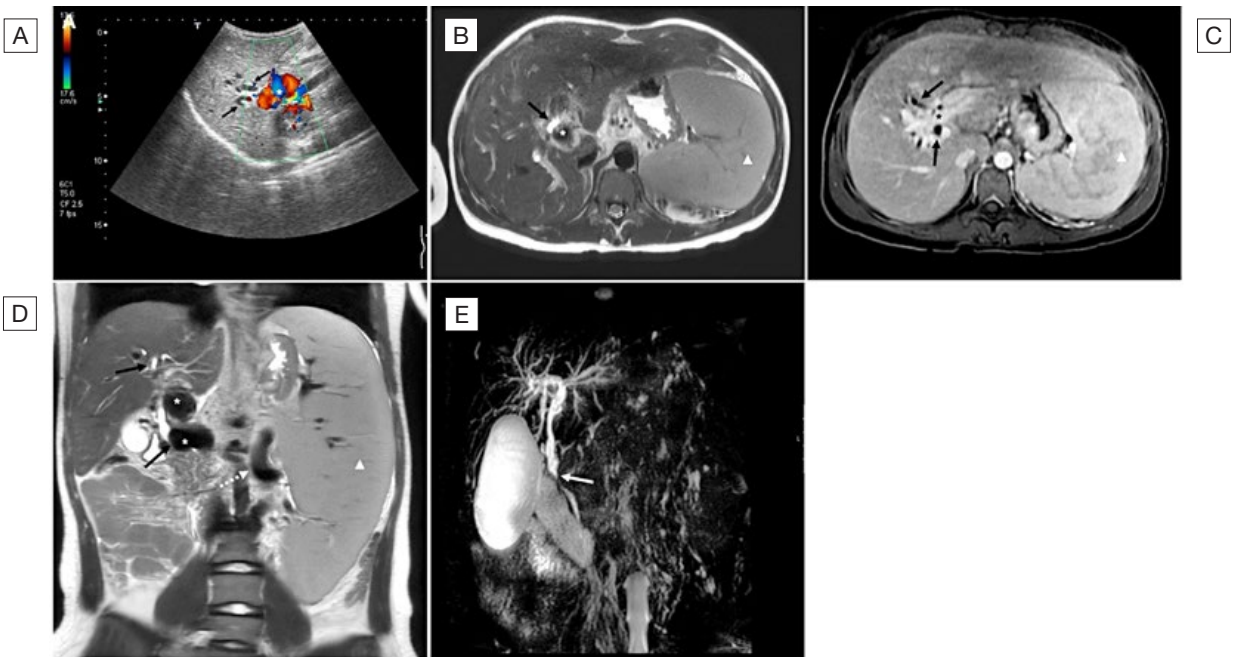

Figure 6: Portal cavernoma and biliary cholangiopathy in an 18-year-old woman due to portal vein thrombosis at 6 years of age. Color Doppler ultrasound [**A**] demonstrates serpiginous porto-portal collateral vessels at the hepatic hilum, corresponding to portal cavernoma (*). Also, there is dilatation of the bile ducts (arrows). Axial T2-weighted [**B**] and portal venous phase T1-weighted [**C**] MRI images demonstrate serpiginous porto-portal collateral vessels consistent with cavernous transformation of the portal vein (*), causing extrinsic compression of the biliary tree with bile duct dilatation (arrows), compatible with biliary cholangiopathy. Massive splenomegaly (▲), secondary to portal hypertension, is present. Coronal T2-weighted image [**D**] shows the same findings. The splenic vein is dilated (dashed arrow). Note that the liver maintains normal morphology and smooth contours. MR cholangiopancreatography (MRCP) [**E**] demonstrates stenosis of the common bile duct (arrow) due to extrinsic compression by the cavernoma [**D***], with upstream biliary dilatation (arrow).

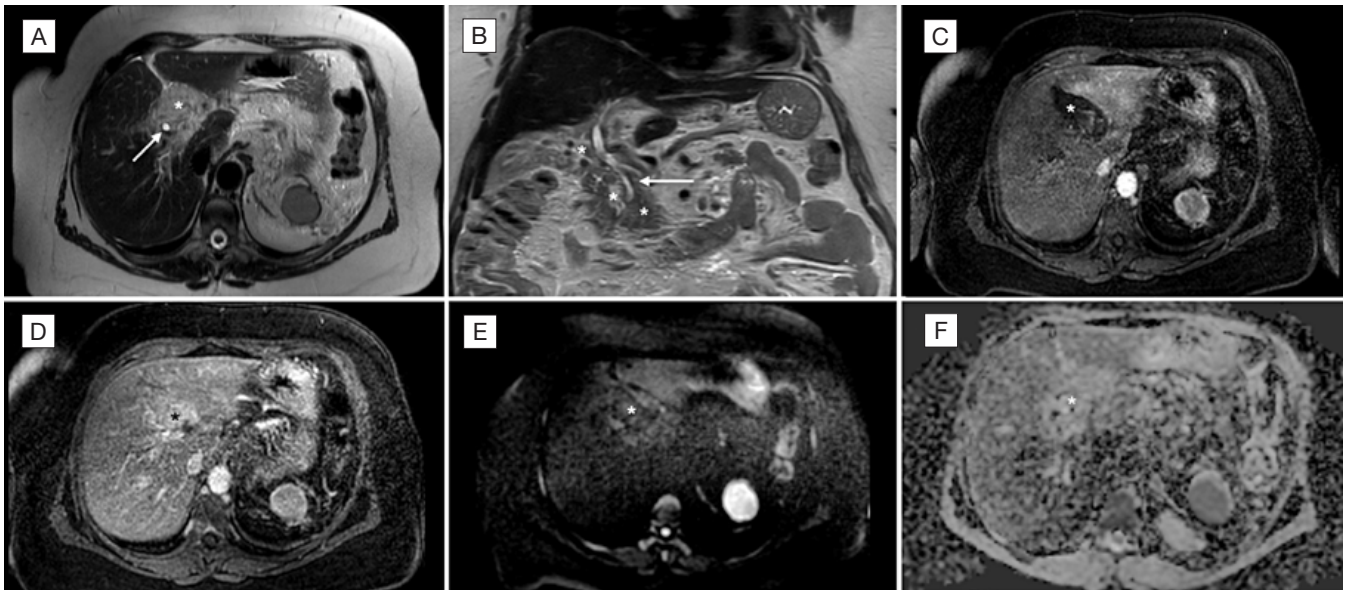

Figure 7: Mass-like portal cavernoma. Axial [**A**] and coronal [**B**] T2-weighted MRI images demonstrate a hyperintense mass-like portal cavernoma (*) with encasement of the common bile duct, resulting in biliary dilatation (arrow). Axial dynamic contrast-enhanced MRI images in the arterial phase [**C**] show heterogeneous hepatic parenchymal enhancement, with areas of hyperenhancement, due to transient hepatic attenuation differences (THAD), predominantly in the left hepatic lobe. The portal venous phase [**D**] demonstrates enhancement of the cavernoma (*). Cavernoma with a mass-like appearance can mimic hepatic hilum tumours, such as cholangiocarcinoma. The absence of diffusion restriction on diffusion-weighted images (DWI) ([**E**], b1000; [**F**], ADC map) is an important clue to differentiate a mass-like cavernoma from hilar cholangiocarcinoma. Furthermore, the liver shows mild left lobe hypertrophy with smooth, regular contours, which helps differentiate non-cirrhotic cavernoma from cirrhosis-related cavernoma.

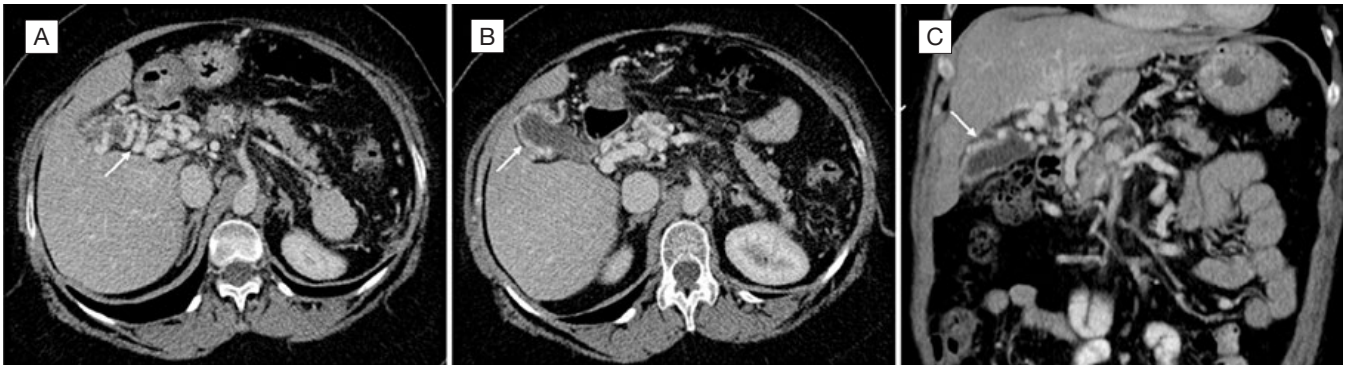

Figure 8: **Portal cavernoma with gallbladder collateral circulation.** Axial [**A** and **B**] and coronal [**C**] contrast-enhanced CT images in the portal venous phase demonstrate peri-gallbladder collateral vessels within the gallbladder wall (arrow), related to portal hypertension. These collateral veins may mimic gallbladder wall thickening with hyperenhancement, potentially simulating gallbladder wall thickening due to inflammatory or neoplastic disease. Recognition of this finding is essential to avoid misdiagnosis, particularly in patients with chronic portal vein thrombosis.

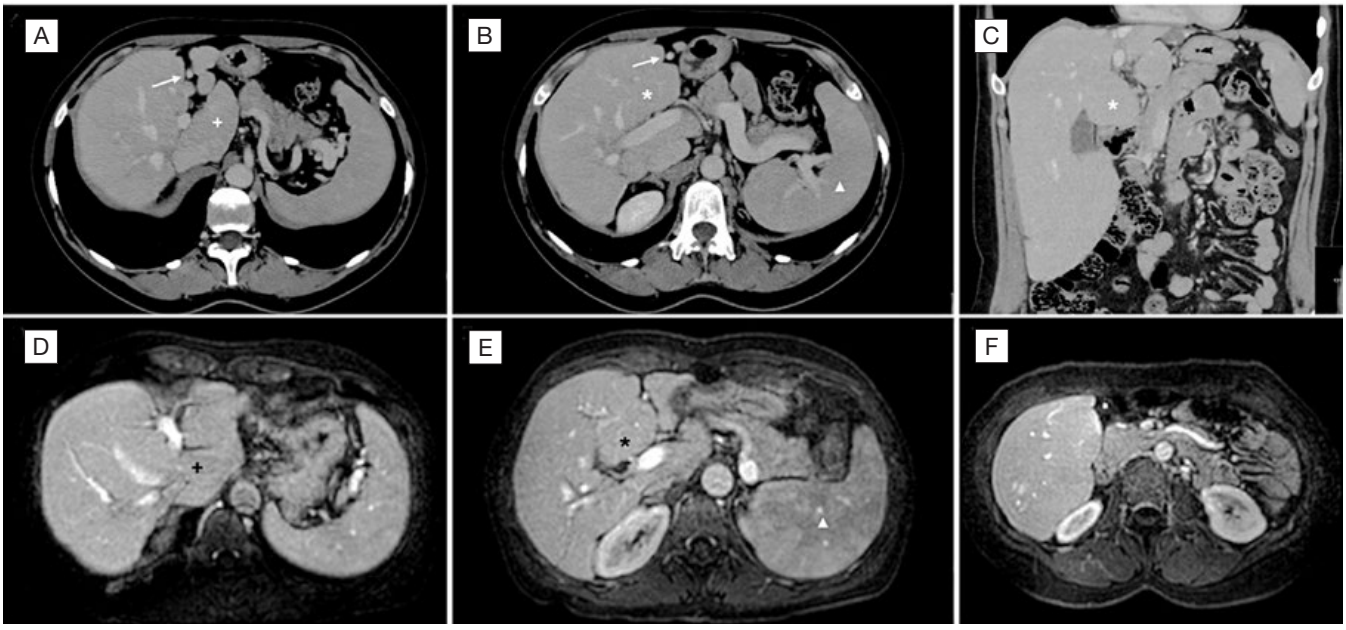

Figure 9: **Porto-sinusoidal vascular disease (PSVD).** Axial [**A** and **B**] and coronal [**C**] contrast-enhanced CT images in the portal venous phase demonstrate hepatomegaly with liver dysmorphia, characterised by hypertrophy of the caudate lobe (+) and segment IV (*), associated with atrophy of the left lateral segments. Despite these morphological changes, the hepatic surface remains smooth and non-nodular. The hepatic veins are patent, and the portal-splenic confluence is patent but dilated. There is repermeabilization of the paraumbilical vein (arrow) and splenomegaly (▲) due to portal hypertension. Axial dynamic contrast-enhanced MRI images [**D** and **F**] show similar liver dysmorphic features, with regular and smooth contours, and signs of portal hypertension. The diagnosis of PSVD was confirmed by hepatic hemodynamic studies and percutaneous liver biopsy. Angiography demonstrated intrahepatic venous collateralization, supporting the diagnosis of PSVD.

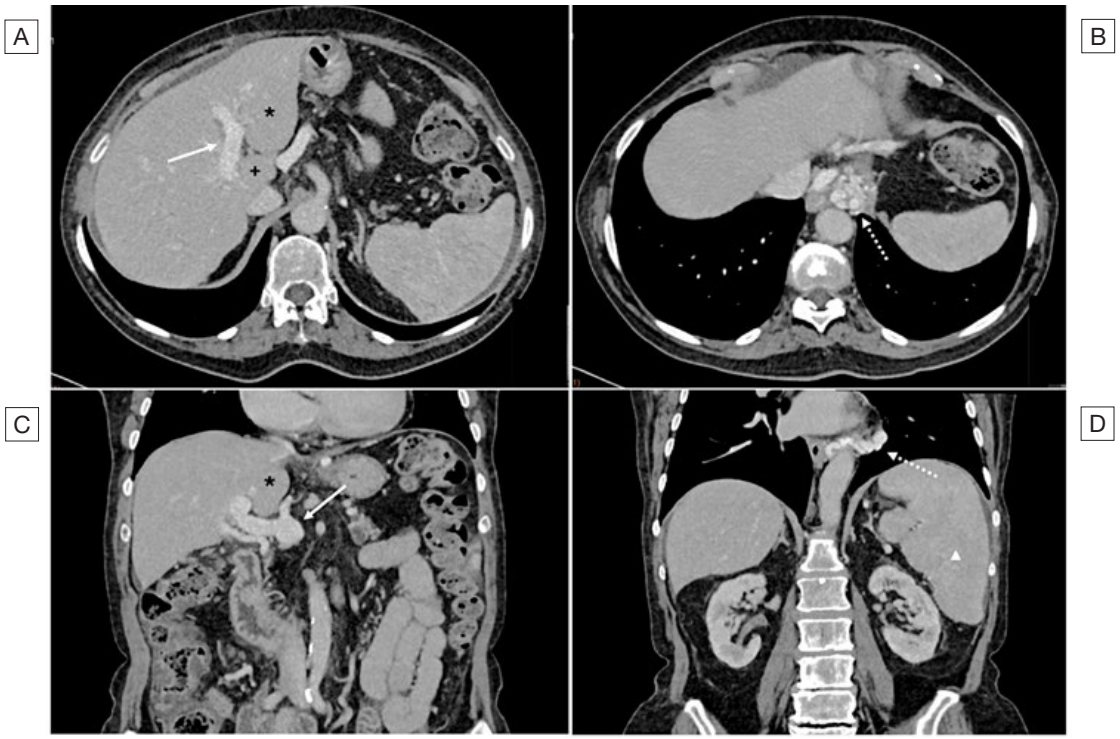

Figure 10: **Porto-sinusoidal vascular disease (PSVD).** Axial [**A** and **B**] and coronal [**C** and **D**] contrast-enhanced CT images in the portal venous phase demonstrate a dysmorphic liver, with hypertrophy of the left lobe (*) and the caudate lobe (+), with atrophy of the right hepatic lobe. Despite these morphological changes, the liver surface remains smooth and non-nodular. Imaging signs of portal hypertension are present, including splenomegaly (▲) and paraesophageal varices (dashed arrows). The portal vein is dilated (arrow), without thrombosis. These findings suggested non-cirrhotic portal hypertension, and the diagnosis of PSVD was confirmed by liver biopsy.

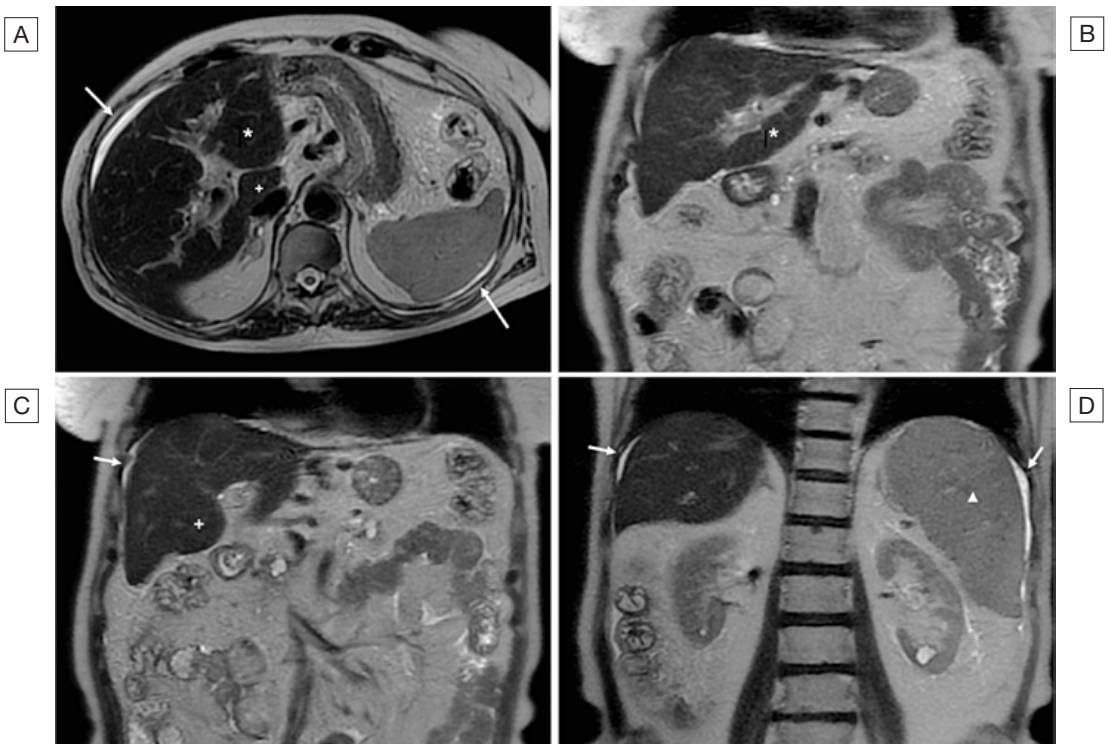

Figure 11: **Porto-sinusoidal vascular disease (PSVD).** Axial [**A**] and coronal [**B-D**] T2-weighted MRI images demonstrate hepatomegaly with liver dysmorphia, characterised by hypertrophy of segment IV (*) and the caudate lobe (+), associated with atrophy of the left lateral segments. Despite these morphological changes, the liver surface remains smooth and non-nodular. Signs of portal hypertension are seen, as splenomegaly (▲) and ascites in the perihepatic and perisplenic spaces (arrow).

Figure 12: **Non-obstructive sinusoidal dilatation due to anticonceptive use.** Axial contrast-enhanced CT images in the arterial phase [**A**] demonstrate patchy and irregular hepatic enhancement, with peripheral hypoenhancing areas, resulting in a mosaic perfusion pattern (arrows). In the axial portal venous phase [**B**], hepatic enhancement becomes more homogeneous, reflecting the transient nature of the perfusion abnormalities. Coronal arterial-phase contrast-enhanced CT image [**C**] also depicts these enhancement alterations.

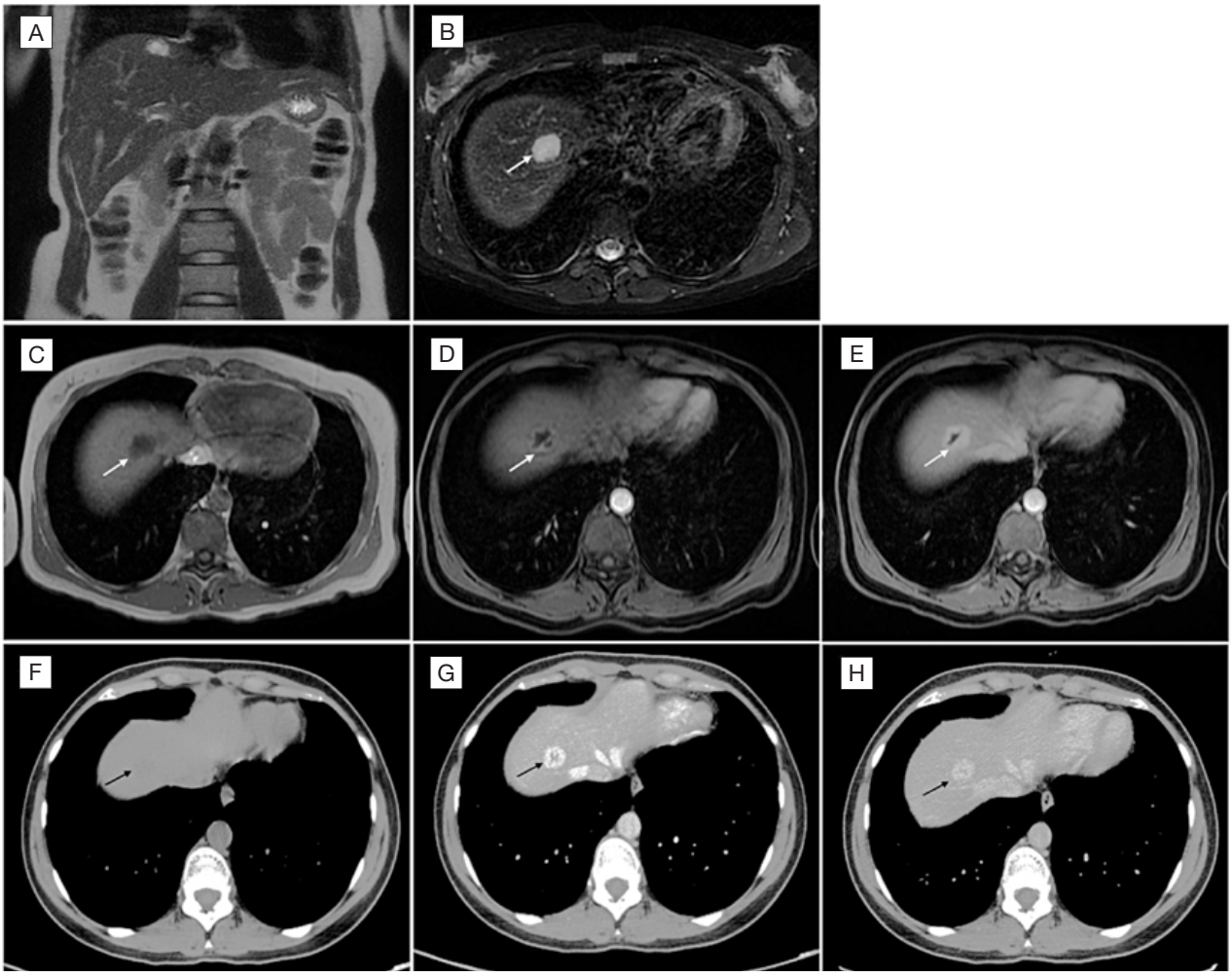

Figure 13: **Peliosis hepatis in a 36-year-old woman with Castleman disease, treated with rituximab for several years.** Coronal T2-weighted MRI image [**A**] shows hepatomegaly with left hepatic lobe hypertrophy. A lesion in segment VIII (arrow), appearing mildly hyperintense on fat-suppressed T2-weighted images [**B**] and hypointense on T1-weighted images [**C**], is seen. On dynamic contrast-enhanced MRI, the lesions demonstrate peripheral rim-like enhancement in the arterial phase [**D**], with centripetal progression of enhancement in the portal venous phase [**E**]. Axial CT images [**F**] - pre-contrast; [**G**] - arterial phase and [**H**] - portal venous phase show the same lesion, which is spontaneously hypodense and demonstrates centripetal enhancement. Although peliotic lesions classically show centrifugal enhancement, centripetal enhancement may also be observed. This should not be misdiagnosed with centripetal enhancement of hepatic hemangioma, which is globular and discontinuous, rather than continuous as in this lesion. Percutaneous liver biopsy was done, which confirmed the diagnosis of peliosis hepatis. Hepatomegaly with left hepatic lobe hypertrophy is also noted.

Figure 14: **Hepatic congestion secondary to cardiac failure.** Axial [**A**] and coronal [**B**] contrast-enhanced CT images in the portal venous phase demonstrate heterogeneous hepatic parenchymal enhancement, with linear and reticular hypoenhancing areas, predominantly in the peripheral regions of the liver, producing the characteristic "nutmeg" appearance or mosaic perfusion pattern, consistent with hepatic congestion. Pleural effusions (+) and cardiomegaly with left ventricle dilation (**) were also seen ([**C**], axial contrast-enhanced CT).

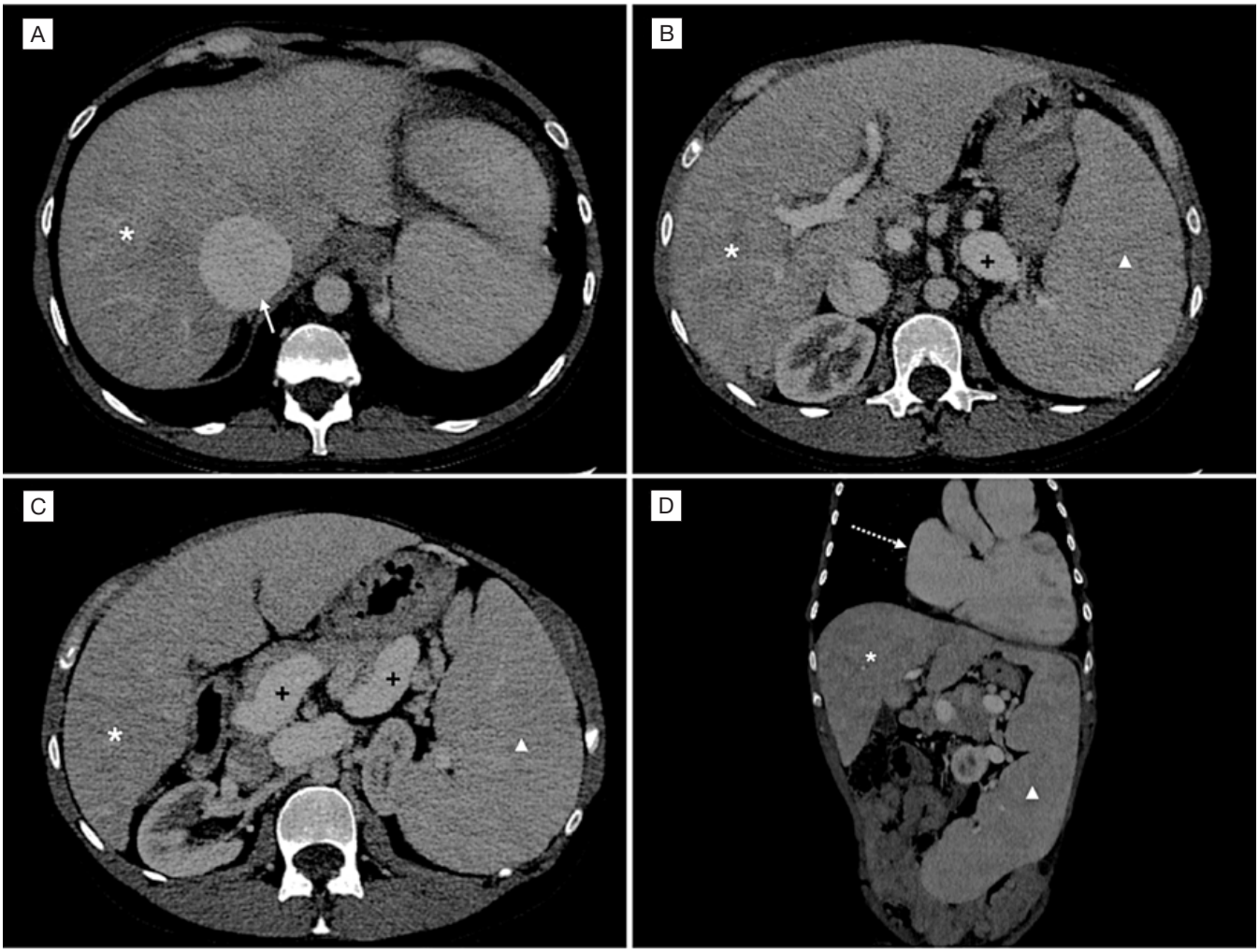

Figure 15: **Hepatic congestion secondary to right heart failure in a patient with idiopathic pulmonary hypertension.** Axial contrast-enhanced CT images in the late arterial phase [**A - C**] demonstrate early enhancement of a dilated inferior vena cava (IVC) (arrow), due to retrograde reflux of contrast material from the right atrium into the IVC. Associated hepatomegaly is present, with heterogeneous parenchymal enhancement and peripheral reticular hypoattenuating areas, consistent with hepatic congestion (*). Additional findings include dilatation of the splenoportal axis (+) and massive splenomegaly (▲), related to portal hypertension. Cardiomegaly with marked right atrial dilatation (dashed arrow) is also evident [**D**], supporting the diagnosis.

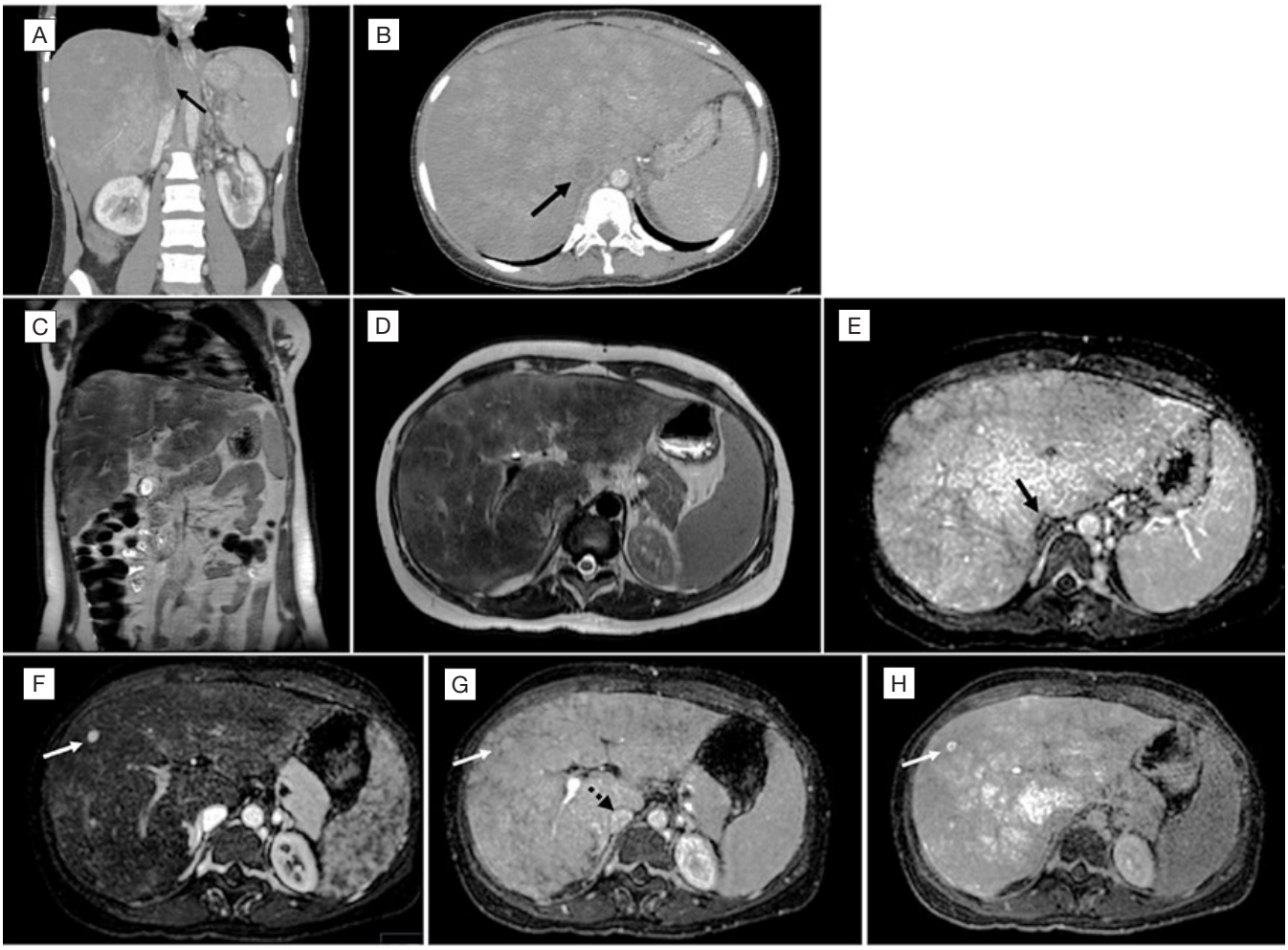

Figure 16: **Budd-Chiari syndrome (BCS) with hyperplasia-like nodules.** Coronal [**A**] and axial [**B**] contrast-enhanced CT images in the portal venous phase demonstrate acute thrombosis of the inferior vena cava (IVC) (arrow). Hepatomegaly is present, with reticular hypoenhancing areas producing a characteristic "nutmeg" appearance, consistent with acute hepatic venous outflow obstruction. Two years later, the patient underwent an MRI examination. Coronal [**C**] and axial [**D**] T2-weighted MRI images demonstrate hepatomegaly, with atrophy of the peripheral hepatic parenchyma and hypertrophy of the central liver regions and caudate lobe. After contrast administration, the hepatic parenchyma shows reticular enhancement, predominantly at the liver periphery, producing a characteristic mosaic perfusion pattern, typically seen in Budd-Chiari syndrome (portal venous phase, [**E**]). On axial dynamic contrast-enhanced MRI, the arterial phase [**F**] demonstrates a hypervascular nodule in segments V/VIII (arrow), which persists as hyperintense on the portal venous phase [**G**] and shows hyperintensity on the hepatobiliary phase [**H**]. These imaging features are typically seen in hyperplasia-like nodules in the setting of chronic hepatic vascular disease. Note the IVC occlusion in [**E**] (arrow), at a cranial level than in image [**G**], where IVC is permeable (dashed arrow).

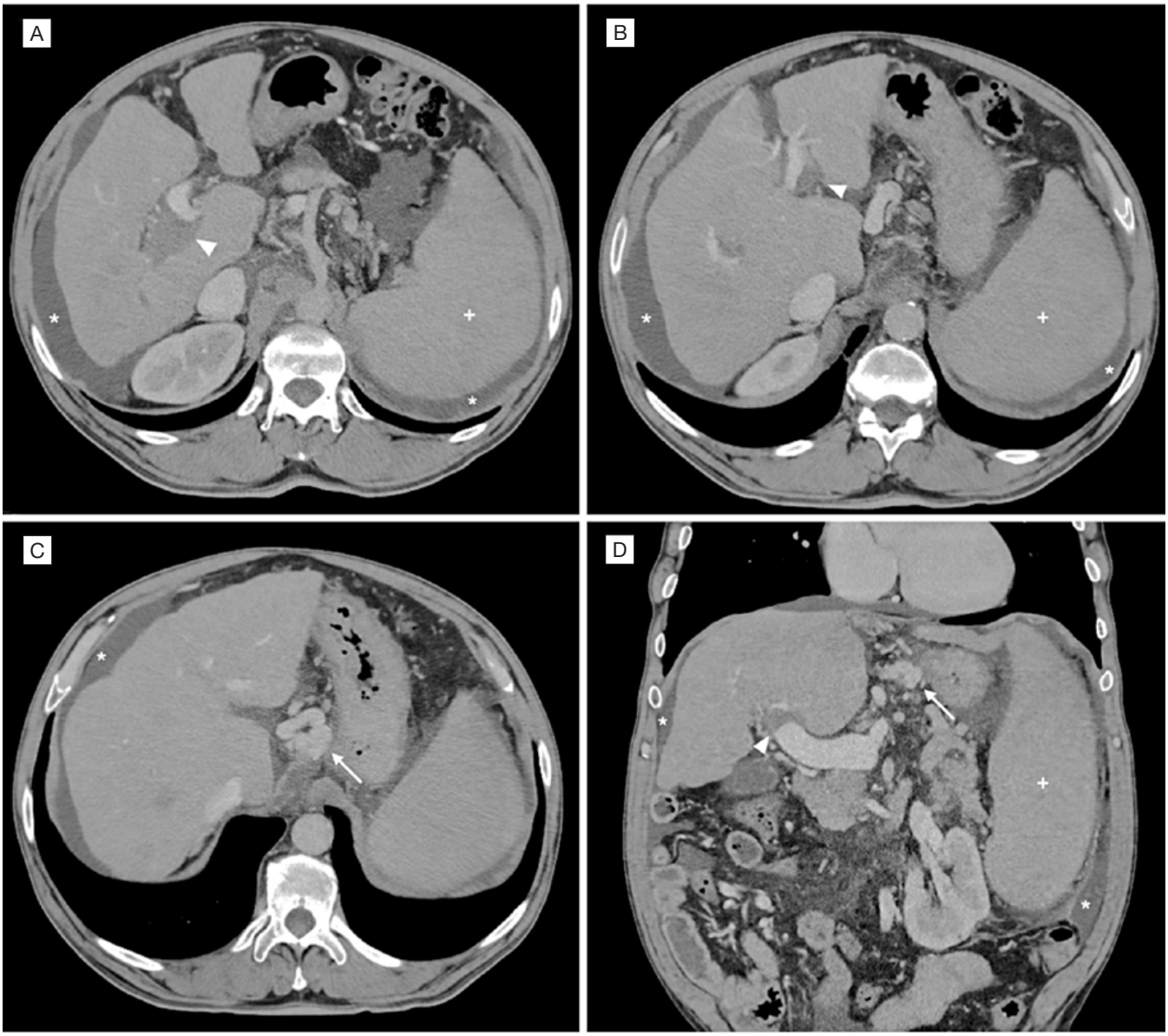

Figure 17: **Acute portal vein thrombosis in the setting of liver cirrhosis.** Axial [**A - C**] and coronal [**D**] contrast-enhanced CT images in the portal venous phase demonstrate acute thrombosis of the right portal vein (arrowhead in **A**) and the left portal vein (arrowhead in **B**). Imaging signs of portal hypertension are present, including splenomegaly (+), paraesophageal varices (arrow), and ascites (*). The liver appears dysmorphic, with hypertrophy of the caudate lobe and left lateral segments and atrophy of segment IV, associated with an irregular hepatic surface. These morphological features are characteristic of liver cirrhosis and help distinguish this entity from non-cirrhotic portal hypertension.

Figure 18: **Cirrhotic liver with portal hypertension.** Axial [**A** and **B**] and coronal [**C**] contrast-enhanced CT images in the portal venous phase demonstrate a dysmorphic liver, with hypertrophy of the left lateral segments (+) and atrophy of segment IV (*). The hepatic surface is nodular and irregular, and parenchymal enhancement is markedly heterogeneous, findings consistent with liver cirrhosis. Associated signs of portal hypertension are present, namely splenic and oesophageal varices (dashed arrows).

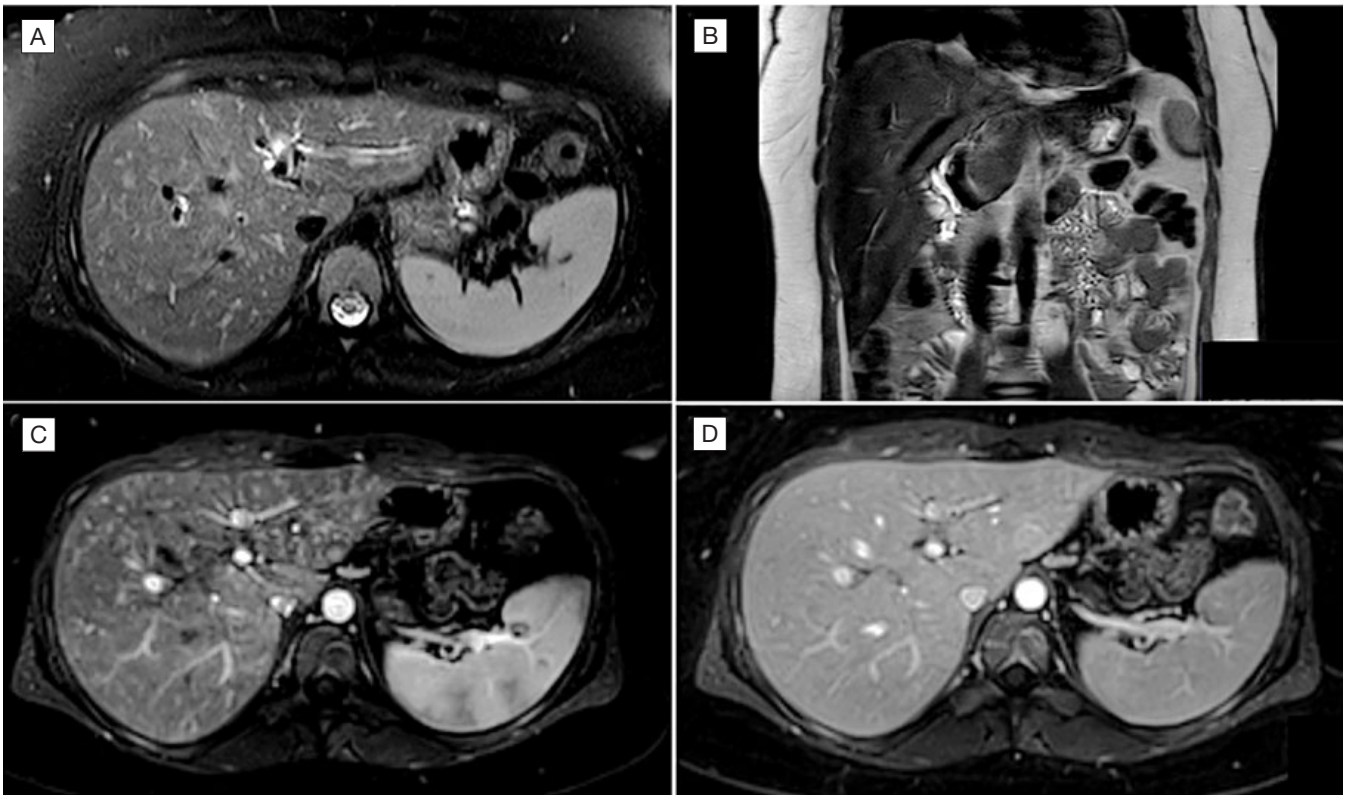

Figure 19: **Primary sclerosing cholangitis with associated hepatitis.** Axial fat-suppressed T2-weighted [**A**] and coronal T2--weighted [**B**] MRI images demonstrate hepatomegaly with preserved liver morphology, smooth contours, and globally homogeneous signal intensity. T2 hyperintensity of the liver parenchyma is noted, likely reflecting inflammatory changes due to hepatitis. Axial arterial phase [**C**] contrast-enhanced MRI image shows heterogeneous hepatic enhancement with transient hepatic arterial intensity changes that become homogeneous on the portal venous phase [**D**]. The preserved liver surface, absence of segmental hypertrophy or atrophy, lack of venous outflow obstruction, and normalisation of enhancement in later phases favour an inflammatory aetiology over primary vascular liver disease.

Contributorship Statement

RT and MF – Study design and manuscript writing, image collection, critical revision, and final approval.
All authors approved the final version to be published.

Declaração de Contribuição

RT e MF – Desenho e escrita do artigo, colheita de imagens, revisão crítica e aprovação final.
Todos os autores aprovaram a versão final a ser publicada.

Ethical Disclosures

Conflicts of Interest: The authors have no conflicts of interest to declare.
Financing Support: This work has not received any contribution, grant or scholarship.
Confidentiality of Data: The authors declare that they have followed the protocols of their work center on the publication of patient data.
Informed Consent: Due to the exclusively illustrative and fully anonymized nature of the images included in this mini-atlas, informed consent was not required. No identifiable patient information is presented, and the material complies with current ethical and editorial standards for publication.
Provenance and Peer Review: Not commissioned; externally peer-reviewed

Responsabilidades Éticas

Conflitos de Interesse: Os autores declaram a inexistência de conflitos de interesse na realização do presente trabalho.
Fontes de Financiamento: Não existiram fontes externas de financiamento para a realização deste artigo.
Confidencialidade dos Dados: Os autores declaram ter seguido os protocolos da sua instituição acerca da publicação dos dados de doentes.
Consentimento: Devido ao caráter exclusivamente ilustrativo e totalmente anónimo das imagens incluídas neste mini-atlas, não foi necessário obter consentimento informado. Não são apresentadas informações que permitam identificar os doentes, e o material cumpre as normas éticas e editoriais vigentes para publicação.
Proveniência e Revisão por Pares: Não comissionado; revisão externa por pares.

Corresponding Author / Autor Correspondente

Manuela França - mariamanuela.franca@gmail.com
Hospital de Santo António, Centro Hospitalar Universitário de Santo António, ULS de Santo António (Santo António), Porto, Portugal
Largo Professor Abel Salazar, 4099-001 Porto, Portugal

Received / Recebido: 08/02/2026
Accepted / Aceite: 25/02/2026
Published online / Publicado online: 15/04/2026
Published / Publicado: 15/04/2026

REFERENCES

1. European Association for the Study of the Liver. European Association for the Study of the Liver. EASL Clinical Practice Guidelines on vascular diseases of the liver. J Hepatol. 2026;84:399-456. doi: 10.1016/j.jhep.2025.08.001.
2. Elkrief L, Hernandez-Gea V, Senzolo M, Albillos A, Baiges A, Berzigotti A, et al. Portal vein thrombosis: diagnosis, management, and endpoints for future clinical studies. Lancet Gastroenterol Hepatol. 2024;9:859-83. doi: 10.1016/S2468-1253(24)00155-9.
3. Rosselli M, Popescu A, Bende F, Al Refaie A, Lim A. Imaging in Vascular Liver Diseases. Medicina. 2024;60:1955. doi: 10.3390/medicina60121955.
4. Brancatelli G, Federle MP, Grazioli L, Golfieri R, Lencioni R. Benign regenerative nodules in Budd-Chiari syndrome and other vascular disorders of the liver: radiologic-pathologic and clinical correlation. Radiographics. 2002;22:847-62. doi: 10.1148/radiographics.22.4.g02jl17847.